

Research Journal of Pharmaceutical, Biological and Chemical Sciences

Synthesis and Characterization of Citrate Capped Au Nanoparticle Dispersion in Liquid Crystalline Compounds.

R K N R Manepalli^{1*}, M Tejaswi¹, M C Rao², G Giridhar³, B T P Madhav⁴, and V G K M Pisipti⁴

¹Department of Physics, The Hindu College, Krishna University, Machilipatnam-521001, India

²Department of Physics, Andhra Loyola College, Vijayawada-520008, India

³Department of Nanotechnology, Acharya Nagarjuna University, Guntur-522510, India

⁴LCRC-R&D, Department of ECE, K L University, Guntur-522502, India

ABSTRACT

In the present manuscript synthesis and characterization are carried out on Liquid Crystalline p-n-nonyloxy benzoic acid (9OBA) compound and with citrate capped 30, 50, 70 & 90 μ l Au nanoparticle dispersion. The polarizing microscopy (POM), Differential Scanning Calorimeter (DSC) technique is used to measure the phase transition temperatures. Further characterization is carried out by various spectroscopic techniques like Scanning Electron Microscopy studies (SEM), Ultra Violet Visible (UV) spectroscopy and Fourier Transform Infra Red Spectroscopy (FTIR). Textural determinations of the synthesized compounds are recorded by using POM connected with a hot stage and camera. The results showed that the dispersion of Au nanoparticles in 9OBA exhibit NC phases as same as the pure 9OBA with reduced clearing temperature as expected. Further, the nematic thermal ranges are also increased while performing both DSC and POM with the dispersion of citrate capped Au nanoparticles. Influence of nanosized Au particles on bonding nature with LC compounds is established.

Keywords: Synthesis, POM, DSC, Nano dispersion, SEM, UV spectroscopy and FTIR.

**Corresponding author*

INTRODUCTION

Liquid Crystals (LCs) are self assembled dynamic functional soft materials which possess both order and mobility at molecular, supra molecular and microscopic levels [1-3]. Liquid Crystals have received much attention in the recent years because they exhibit anisotropy in their mechanical, electrical and optical properties, behaving like solid crystals. Nevertheless, they have no ability to support shearing and thus they flow like ordinary isotropic solutions and have ability to transfer their long range orientation order on the dispersed materials such as nanoparticles and various colloids [4-10]. This dual property nature made these materials important in technological applications such as displays and optical switches. The key point for all the possible applications is the alignment of liquid crystal molecules on the substrate [11, 12]. Different researchers of physics, chemistry and technology have shown interest on liquid crystals due to their multifaceted applications. A variety of applications has been takes place while dispersion of metal nanoparticles in to the moiety of LC. These nano doping materials investigated include metallic nanoparticles [13], semiconducting nanoparticles [14], ferroelectric nanoparticles [15], carbon related nanoparticles [16] and other [17]. Metal nano clusters of gold of size less than 2 nm differentiates them from bulk gold and gold nano crystals. This size effect leads to the discrete electronic structure of the core due to the quantum size effect [18-21]. As these nanoparticles are unstable and form clusters, the capping agent's helps to prevent uncontrollable growth of particles, prevent particle aggregation, control growth rate and controls particle size [22]. Among the variety of stabilizers and protective capping agents for gold nanoparticles, the one commonly used is citrate, which stabilizes the gold nanoparticles through mutual electrostatic repulsion between neighboring gold nanoparticles; this occurs as a result of the negative surface charge of the citrate layer [23]. Rao et al. have presented the results on different oxide materials in their earlier studies [24-30]. Homomorphic filtering technique is also used for digital image enhancement, especially when the input image suffers from poor illumination conditions and this filtering technique has been used in many different imaging applications, including biometric, medical and robotic vision.

EXPERIMENTAL

The LC compound 9OBA is brought from Sigma Aldrich, USA and used as such. The citrate capped Au nanoparticles are synthesized from the citrate reduction process. Hydrogen tetrachloroaurate (III) trihydrate ($\text{HAuCl}_4 \cdot 3\text{H}_2\text{O}$) ACS, 99.99 % and trisodium citrate dehydrate ($\text{Na}_3\text{C}_6\text{H}_5\text{O}_7 \cdot 2\text{H}_2\text{O}$) 99 % are purchased from Sigma Aldrich Laboratories. 20 ml of 1 mM Auric chloride is heated and then 2 ml of 1 % tri-sodium citrate is added drop by drop and stirred vigorously. Then the solution changed gradually from transparent light yellow, dark black and finally to the characteristic wine red, which indicated the formation of citrate capped Au nanoparticles. For uniform dispersion of nanoparticles into 9OBA, 30 μl of aqueous solution of citrate capped Au nanoparticles first dissolved in toluene, stirred well about 45 minutes and later introduced in the isotropic state of LC material (9OBA) and stirred well about three hours. The same process is repeated with the dispersion of 50 μl , 70 μl and 90 μl separately. After cooling, the nanocomposite 9OBA is subjected to study of the textural and phase transition temperatures using a Polarizing Optical Microscope (SDTECHS make) with a hot stage in which the substance was filled in planar arrangement in 4 μm cells and these could be placed along with the thermometer described by Gray [31]. Textural and phase transition temperatures are studied after preparation of the sample and observations are made again to understand the stability of Au nanoparticles. A DSC (Perkin Elmer Diamond DSC) was used to obtain the transition temperatures and the enthalpy values. This DSC can be used for exothermic as well as endothermic regimes. FTIR is a powerful tool for identifying types of chemical bond in a molecule by producing an IR absorption spectrum and useful for identifying chemicals that are either organic or inorganic. BRUKER-ALPHA FTIR spectrometer is used in the present study. The presence of Au nanoparticles in 9OBA is studied by SEM- EDAX data.

RESULTS AND DISCUSSION

Phase transition temperatures and phase sequence of the compounds has been presented by POM and confirmed by DSC. The existence of dispersed nanoparticles and their size determined by UV, FTIR and SEM techniques.

Polarizing Optical Microscope: The transition temperatures and textures observed at 10X (SP - Achro) magnification by Polarizing Microscope in pure 9OBA is shown in Figure-1(a-c) while that of 9OBA with

dispersed with citrate capped Au nanoparticles in 30, 50 and 90 μl concentrations shown in Figure-2(a-c), Figure-3(a-c) and Figure-4(a-c), respectively. The thermal ranges of nematic and smectic C phases are changed slightly due to the dispersion of nanoparticles and the textures of the phase's changes by the self assembly of nanoparticles. The DSC thermograms are shown in the Figure-(5-7). The transition temperatures and enthalpy changes at the phase transformations determined through POM and DSC as shown in the Table-1 and Figure-8. It is observed that the transition temperatures are lower and nematic thermal ranges increased while 30, 50, 70 and 90 μl concentrations Au nanoparticles dispersed in 9OBA.

Table 1: Phase variants, transition temperatures, Enthalpy values of 9OBA pure and with dispersed 30, 50, 70 & 90 μl Au nanoparticles

S. No.	Compound	DSC/POM	Scan Rate	Transition Temperatures $^{\circ}\text{C}$				Thermal Ranges	
				I-N	N-SmC	SmC-SolidI	SolidI – Solid II	Δn	ΔS_{mc}
1	9OBA PURE	DSC	20c/min $\Delta HJ/g$	132.52 14.34	115.38 4.57	89.35 30.78	64.98 58.15	17.14	26.03
		POM		132.9	116.0	91.0	63.0	16.9	25
2	9OBA+30 μl of ct AU	DSC	20c/min $\Delta HJ/g$	124.79 5.4456	110.31 3.4112	88.50 34.2918	64.73 57.7150	14.48	21.81
		POM		126.4	109.7	85.5	66.7	16.7	24.2
3	9OBA+50 μl of ct AU	DSC	20c/min $\Delta HJ/g$	134.03 1.215	112.61 3.4878	89.14 23.3695	65.22 35.0888	21.42	23.47
		POM		135.4	109.6	86.0	66.5	25.8	23.6
4	9OBA+70 μl of ct AU	DSC	20c/min $\Delta HJ/g$	131.4	112.98 4.27	87.92 34.84	66.84 53.04	18.42	25.06
		POM		132.2	112.5	86.8	67.5	19.7	25.7
5	9OBA+90 μl of ct AU	DSC	20c/min $\Delta HJ/g$	129.77 3.5138	113.30 3.3368	89.18 22.8475	65.69 47.4670	16.47	24.12
		POM		128.6	112.4	88.6	70.6	16.2	23.8

Textures of 9OBA Pure

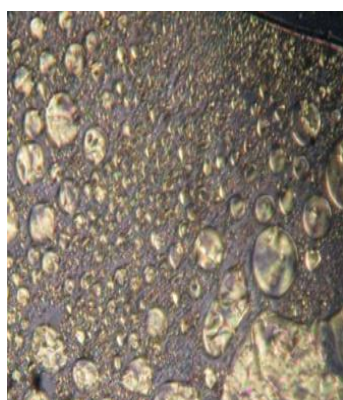


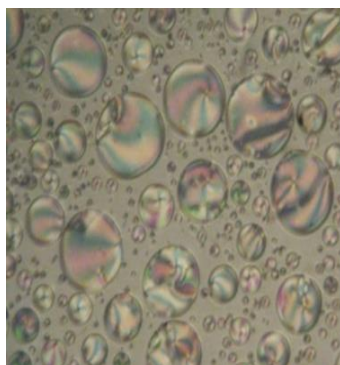
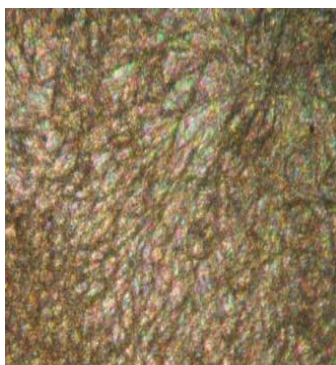
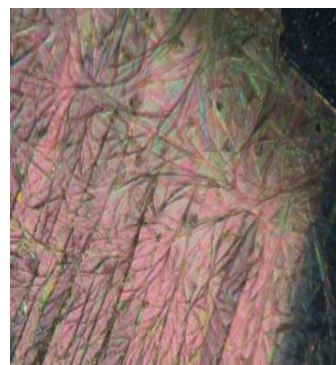
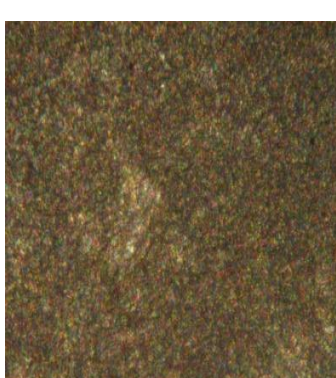
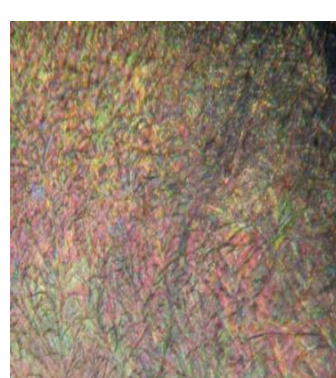
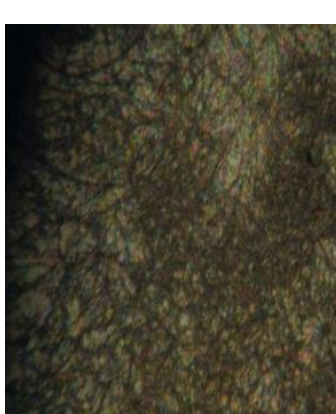
Figure-1a: nematic droplets at 116.0 $^{\circ}\text{C}$



Figure-1b: smectic C at solid 91 $^{\circ}\text{C}$



Figure-1c: smectic-c at 132.8 $^{\circ}\text{C}$

Textures of 9OBA+ 30 μ l Au nanoparticlesFigure-2a: nematic
at 66.7°CFigure-2b: smetic-c
at 109.7°CFigure-2c: solid
at 131.5°CTextures of 9OBA + 50 μ l of Au nanoparticlesFigure-3a: nematic-
at 109.6°CFigure-3b: smetic-c
at 109.4°CFigure-3c: Smetic-solid-1
at 86.5°CTextures of 9OBA+ 90 μ l of Au nanoparticlesFigure-4a: pure nematic
at 126.5°CFigure-4b: smetic-c
at 112.4°CFigure-4c: solid-I
at 188.6°C

DSC Thermograms

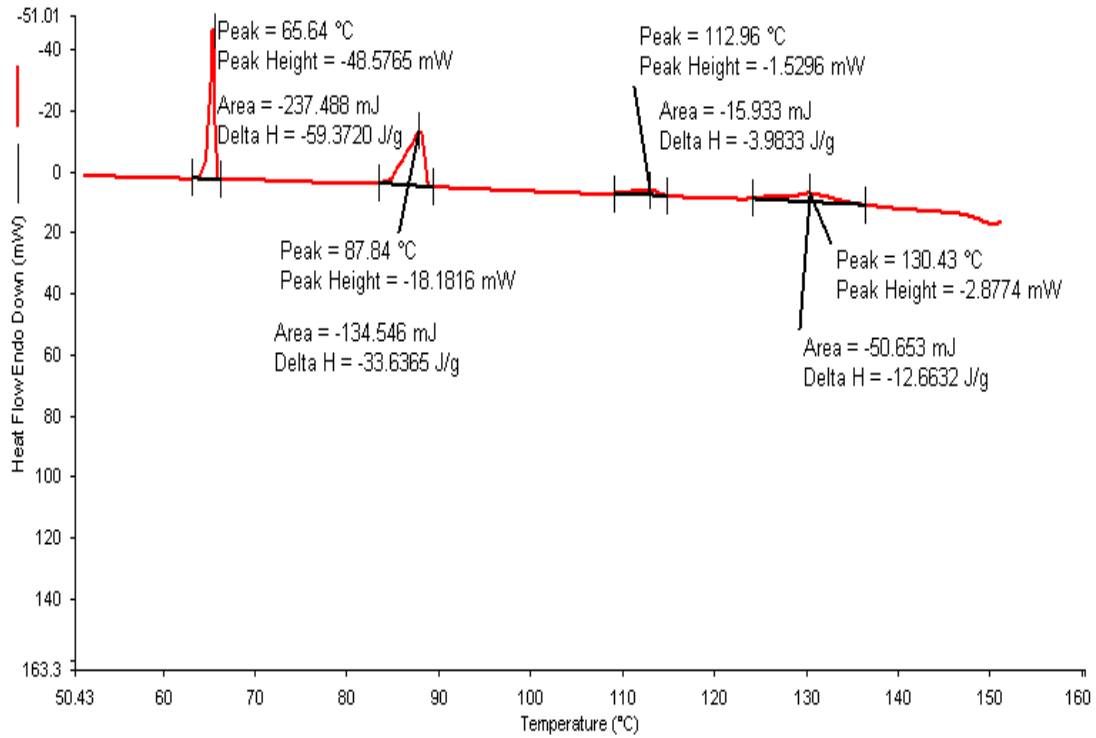


Figure-5: DSC Thermogram of 9OBA + 30 µl Au nanoparticles

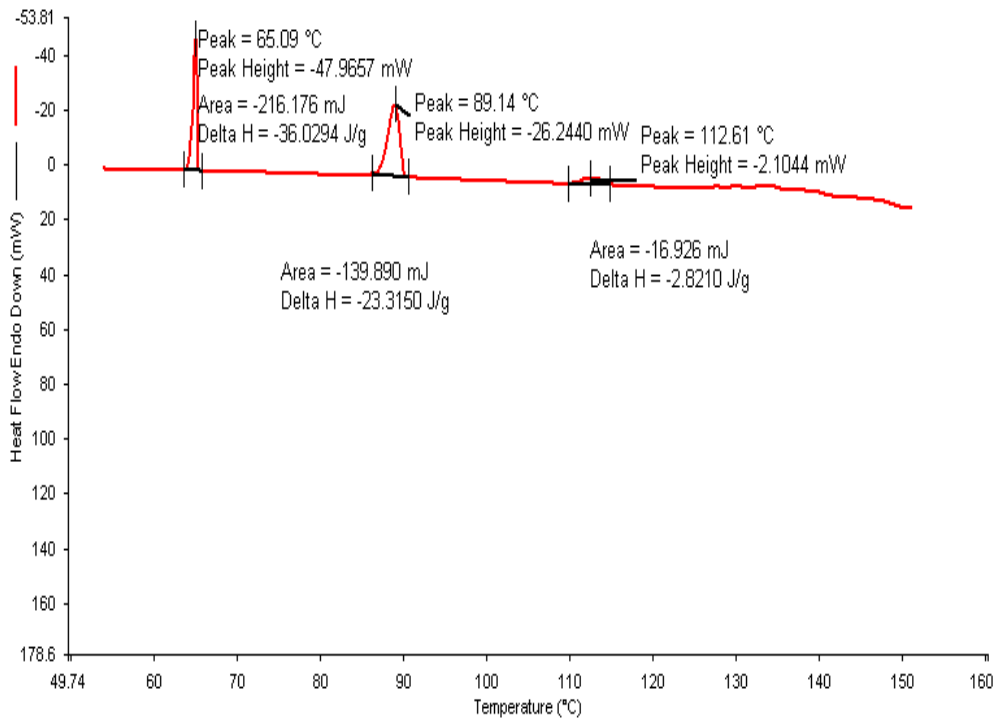


Figure-6: DSC Thermogram of 9OBA + 50 µl citrate capped Au nanoparticles

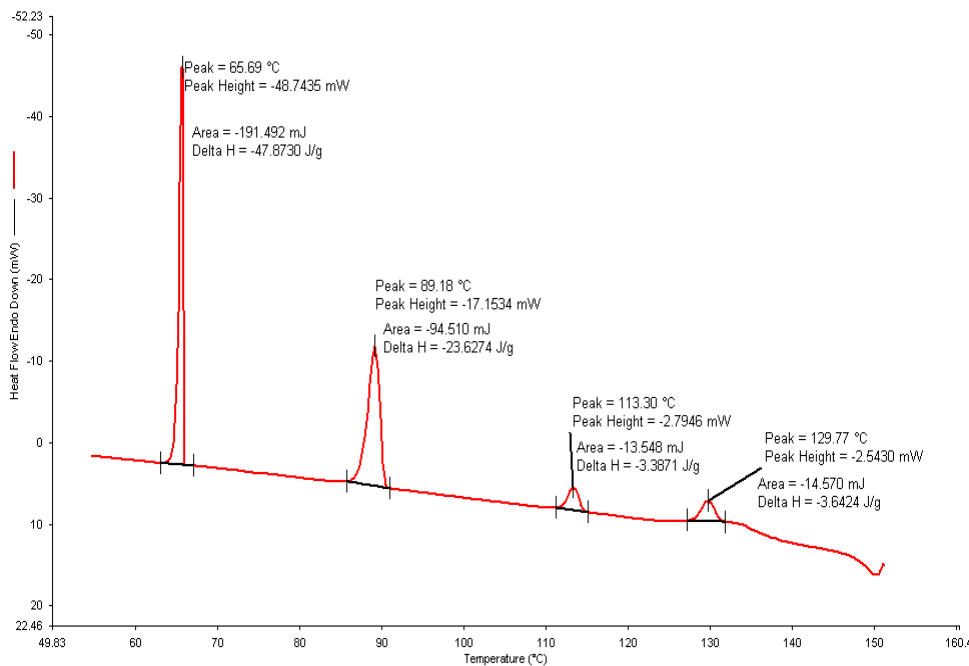


Figure-7: DSC Thermogram of 9OBA + 90 µl citrate capped Au nanoparticles

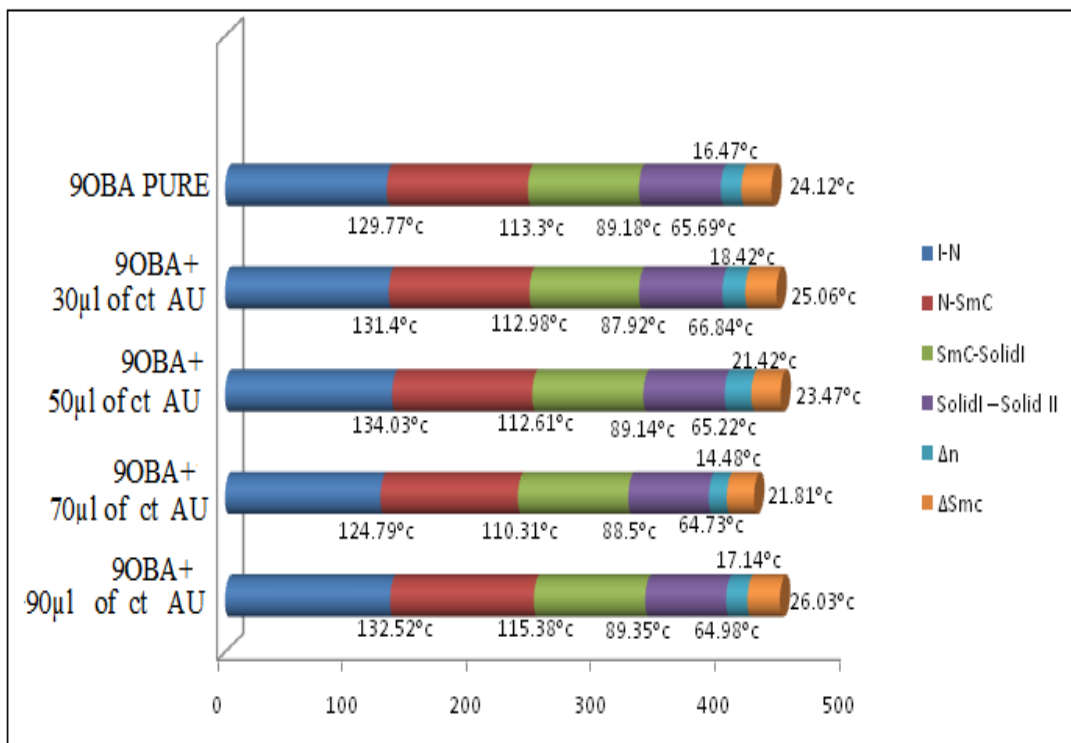


Figure-8: Temperature ranges of nematic and smectic regions of 9OBA

Ultraviolet –Visible (UV) Spectroscopy

The Figure-9 shows the UV-visible spectra of pure citrate capped gold nanoparticles and citrate capped Au nanoparticles doped 9OBA LC sample. It is observed that the spectrum for pure 9OBA does not exhibit any absorption peaks in the wavelength range of 500–650 nm. However, the spectrum of nano doped

9OBA shows the significant peak at 550 nm, which are the characteristic peak of Citrate capped Au nanoparticles. So, the UV-visible spectral study confirms the presence of Citrate capped Au nanoparticles in the prepared nano doped LC.

FTIR Analysis

FTIR is used to analyze presence of functional groups in molecule and presence of dopants is represented by the change in the transmittance as shown in the spectrum. As synthesized citrate capped Au nanoparticles dispersed in 9OBA compound is analyzed by using FTIR at room temperature. The compound is stable at room temperature, so a small amount of compound is taken directly for the spectral recording by using ATR (Attenuated Total Reflectance) technique and the IR frequencies in solid state which are correlated in bond with the pure bond 9OBA. The assigned bonds corresponding to the resultant frequencies from the spectra are tabulated (Table-2). Due to the excitation of both molecular vibrations and rotations absorptions of electromagnetic radiation causes the formation of absorption bands in the IR spectra which are useful to explain the bonding interaction of the molecules. In both spectra exhibit a strong electromagnetic absorption at 1670.54 cm^{-1} , 1605.84 cm^{-1} and 1252.05 cm^{-1} , 1257.88 cm^{-1} corresponding to aromatic ring stretching. The absorption bands at 2913.76 cm^{-1} and 2916.09 cm^{-1} , correspond to OH bond. The existence of OH bond vibration at 646.47 cm^{-1} , 643.56 cm^{-1} and also represents the benzoic acids moiety due to their strong intensity and strongly supports the existence of 9OBA. The bond 842.89 cm^{-1} , 842.89 cm^{-1} are assigned to stretching ring vibration at the out of plane. While dispersing the citrate capped Au nanoparticles the intensity of the peaks are found to be decreased as shown in the Figure-10. The intensity of 9OBA with dispersed nanoparticles is found to increase, this is related to the change in dipole that occurs during the vibration [32]. The vibrations that produce small change in dipole result in a less intense absorption than those that result in a relatively modest change in dipole.

Table 2: Functional group intensities for 9OBA pure and with dispersed citrate capped Au nanoparticles across the following wavelengths

S.No	Wavenumber cm^{-1}	Intensity for pure LC	Intensity for LC with dispersed citrate capped Au nanoparticles	Functional Group
1	2913.76	0.7723	0.8251	OH bond
2	1667.63	0.6937	0.7735	Benzoic acid
3	1608.75	0.6778	0.7699	Ring stretching
4	1577.86	0.8361	0.8815	
5	1513.17	0.8729	0.9208	
6	1465.37	0.8642	0.9072	
7	1429.24	0.8643	0.8754	
8	1330.73	0.8263	0.8717	dimer
9	1254.96	0.5611	0.6888	Aromatic ring structure
10	1171.04	0.7183	0.7956	CHOH bending vibration
11	842.89	0.7563	0.8239	Ring out of plane pplane
12	767.12	0.7084	0.7784	Aromatic ring stretching
13	719.32	0.8876	0.9221	CH out of plane
14	691.35	0.8705	0.9085	C=O bending
15	646.65	0.7171	0.7907	OH bond

SEM Analysis

A small amount of Au nanoparticles and nanoparticles dispersed LC compounds are taken on sample holder for the scanning electron microscopy. The SEM provides the investigator with a highly magnified image of the surface of a material as the present sample contains electrons; which are needed for getting SEM image. The resolution of the SEM can approach a few nm and it can operate at magnifications that are easily adjusted from about 10×-300,000×. SEM gives not only topographical information but also gives the information regarding the composition of the elements in the material [33, 34]. The EDS and SEM images of citrate capped Au nanoparticles and with the dispersion of 50 μl citrate capped Au nanoparticle in 9OBA is shown in the Figure-11 and Figure-12. It is clear from Figure-12 that the nanoparticles are in the sizes of 29-50 nm. From EDS data shown in Figure-11 elucidates the presence of nanoparticles in the compound is well established.

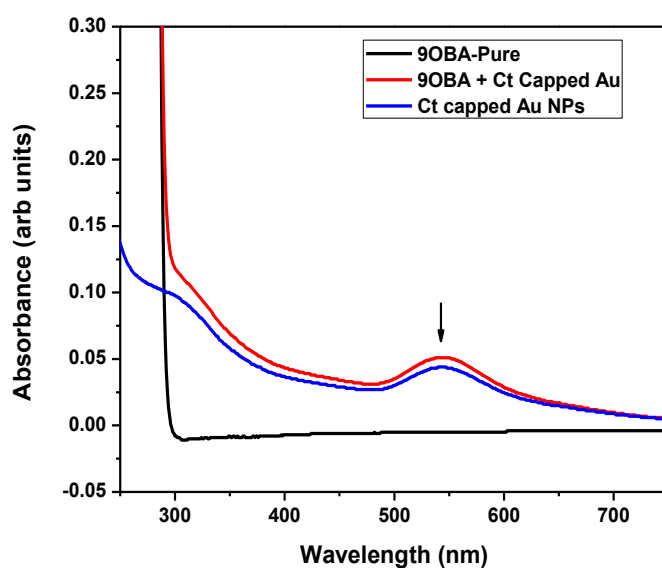


Figure-9: UV-visible spectra of pure 9OBA, pure and citrate capped Au nanoparticles dispersed in 9OBA

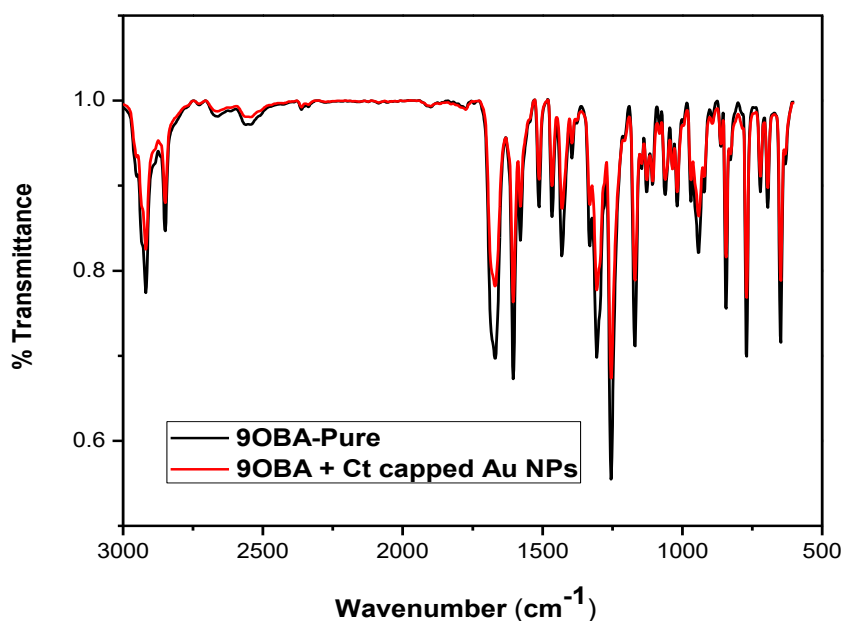


Figure-10: FTIR of 9OBA pure and with dispersed 50 μ l citrate capped Au nanoparticles

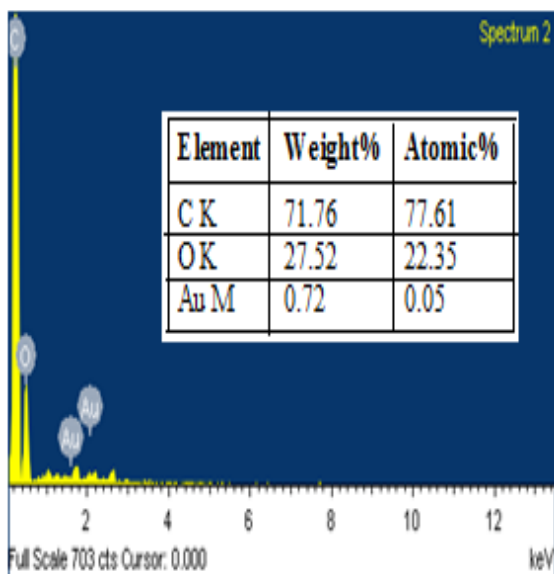


Figure-11: EDS data of citrate capped Au nanoparticles

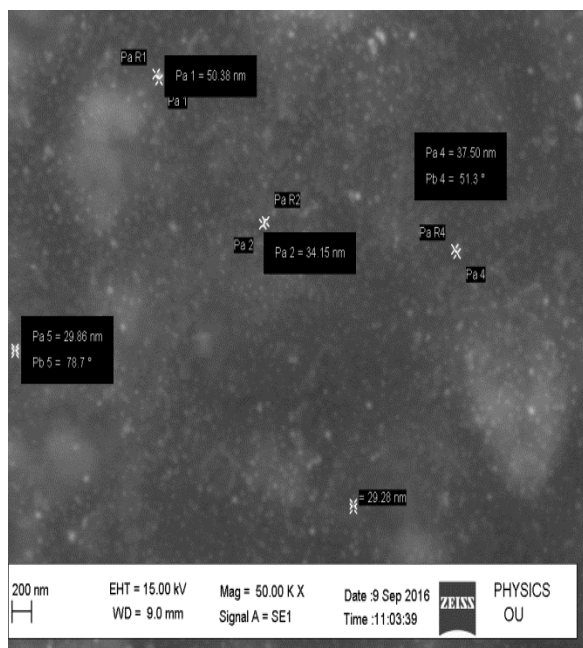


Figure-12: SEM Photograph of citrate capped Au nanoparticles

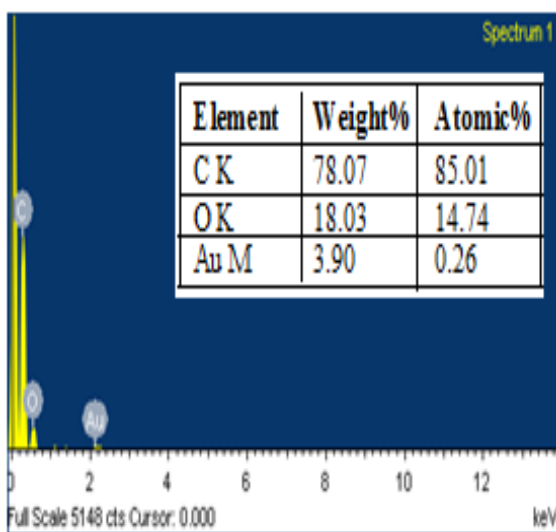


Figure-13: EDS data 9OBA with 50 μ l citrate capped Au nanoparticles

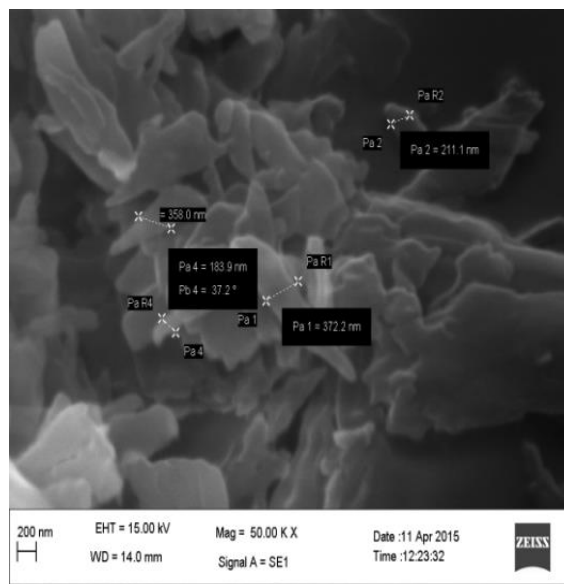


Figure-14: Sem Photograph of 9OBA with 50 μ l citrate capped Au nanoparticles

CONCLUSIONS

With the present results we demonstrated the dispersion of citrate capped Au nanoparticles in LC 9OBA changing of their textures, phase transition temperatures and shifts in vibrational bands by using Polarizing Microscope, Differential Scanning Calorimeter and Fourier Transform Infra Red techniques respectively. The transition temperatures obtained from polarizing microscope are in good agreement with those obtained from DSC. The UV-Visible spectral study confirms the presence of citrate capped Au nanoparticles in the prepared nanodoped LC. The presence of citrate capped Au nanoparticles in LC 9OBA is also confirmed by the EDS data of SEM and the pure gold nanoparticles sizes are in the range of 29-50 nm.

**ACKNOWLEDGEMENTS**

The corresponding author R.K.N.R. Manepalli is thankful to the UGC for grant 42-784/2013 (SR).

REFERENCES

- [1] Kato T, Mizoshita N, Kishimoto K. *Angew Chem Int Ed* 2006; 45: 38-68.
- [2] Goodby JW, Saez IM, Kowling SJ, Gortz V, Draper M, Hall AW, Sita S, Cosquer G, Lee SE, Raynes EP. *Angew Chem Int Ed* 2008; 47: 2754-2787.
- [3] Tschierske C. *Chem Soc Rev* 2007; 36: 1930-1970.
- [4] Shiraishi Y, Toshima N, Maeda K, Yoshikawa H, Xu J, Kobayashi S. *Appl Phys Lett* 2002; 81: 2845-2852.
- [5] Lynch MD, Patrick DL. *Nano Lett* 2002; 2: 1197-1201.
- [6] Dierking I, Scalia G, Morales PJ. *J Appl Phys* 2005; 97: 044309-1.
- [7] Basu R, Iannacchione G. *Appl Phys Lett* 2008; 93: 183105-1.
- [8] Lagerwall JPF, Scalia G. *J Mater Chem* 2008; 18: 2890-2898.
- [9] Russell JM, Oh S, LaRue I, Zhou O, Samulski ET. *Thin Solid Films* 2006; 509: 53-57.
- [10] Basu R, Iannacchione G. *Phys Rev E* 2009; 106: 124312-1.
- [11] De Gennes PG, Prost J. *The Physics of Liquid Crystals* 1993; second ed., Clarendon, Oxford.
- [12] Takato K, Hasegawa M, Koden M, Itoh N, Hasegawa R, Sakamoto M. Taylor & Francis 2004; New York.
- [13] Shiraishi Y, Toshima N, Maeda K, Yoshikawa H, Xuland K, *Applied Phys Lett* 2002; 81: 2845-2847.
- [14] Chen WT, Chen PS, Chao CY. *Jpn J Appl Phys* 2009; 48: 015006.
- [15] Reznikov Y, BuChnev O, Tereshchenko O, Reshetnyak V, Glushchenko A, West J. *Phys Rev Lett* 2003; 82: 1917-1919.
- [16] Lee W, Wang CY, Shih YC. *Appl Phys Lett* 2004; 85: 513-515.
- [17] Hirst LS, Kirchoff J, Inman R, Ghosh S. *Proc SPIE* 2010; 76180F-76180F-7.
- [18] Tsukuda TB. *Chem Soc Jpn*.2012; 85: 151-168.
- [19] Price RC, Whetten RL. *J Am Chem Soc* 2005; 127: 13750-13751.
- [20] Qian H, Zhu Y, Jin RP. *Natl Acad Sci* 2012; 109: 696-700.
- [21] Dass A. *J Am Chem Soc* 2011; 133: 19259-19261.
- [22] Hari Krishna B, Sandeep Kumar. *Chem Soc Rev* 2011; 40: 306-319.
- [23] Sugunan A, Dutta J. *Res Soc Symp Proc* 2005; 901: 257-262.
- [24] Rao MC. *Optoelect & Adv Mater (Rapid Commu)* 2011; 5: 85-88.
- [25] Muntaz Begum Sk, Rao MC, Ravikumar RVSSN. *Spectrochim Acta Part A Mol & Biomol Spec* 2012; 98: 100-104.
- [26] Muntaz Begum Sk, Rao MC, Ravikumar RVSSN. *J Inorg Organomet Poly Mater* 2013; 23(2): 350-356.
- [27] Rao MC. *J Optoelect & Adv Mater* 2011; 13: 428-431.
- [28] Rao MC, Hussain OM. *Eur Phys J Appl Phys* 2009; 48(2): 20503
- [29] Rao MC. *Optoelect & Adv Mater (Rapid Commu)* 2011; 5(5-6): 651-654.
- [30] Ravindranadh K, Rao MC, Ravikumar RVSSN. *J Luminesce* 2015; 159: 119-127.
- [31] Gray GW. *Molecular structures and properties of liquid crystals* 1962; Academic press.
- [32] Manepalli RKNR, Giridhar G, Rao MC, Pardhasaradhi P, Sivaram K, Pisipati VGKM. *Carmelight* 2016; 12(1): 91-101.
- [33] Goldstein JI et al. *Scanning Microscopy and X-Ray Microanalysis* 1981; Plenum Press, New York.
- [34] Newbury D et al. *Advanced Scanning electron Microscopy and X-Ray Microanalysis* 1986; Plenum Press, New York.